

Geochemical evolution of rift magmas by progressive tapping of a stratified mantle source beneath the Ross Sea Rift, Northern Victoria Land, Antarctica

A. Rocholl^{a,b,1}, M. Stein^c, M. Molzahn^{a,b}, S.R. Hart^d, G. Wörner^{a,2}

^a *Institut für Geowissenschaften, Universität Mainz, Becherweg 21, D-55099 Mainz, Germany*

^b *Max-Planck-Institut für Chemie, Postfach 3060, D-55020 Mainz, Germany*

^c *Institute of Earth Sciences, The Hebrew University, Givat Ram, Jerusalem, Israel*

^d *Woods Hole Oceanographic Institution, Woods Hole, MA 02543, USA*

Received 5 July 1994; accepted after revision 16 February 1995

Abstract

Source compositions of Neogene–Quaternary volcanic rocks from the McMurdo Volcanic Group of the Ross Sea Rift in Northern Victoria Land, Antarctica are constrained by Nd–Sr–Pb isotopes and trace element ratios in near-primary basalts. The rocks erupted along the western rift margin (Victoria Land Basin) and the western rift shoulder (Transantarctic Mountains). Near-primary basalts show no evidence of crustal contamination, suggesting that their initial Nd–Sr–Pb isotopes reflect the composition of their mantle sources. The initial isotope ratios of near-primary basalts range from about $^{87}\text{Sr}/^{86}\text{Sr} = 0.70281$ to 0.70504 and $^{143}\text{Nd}/^{144}\text{Nd} = 0.51269$ to 0.51291 ($\epsilon_{\text{Nd}(t)} = 1.3$ – 5.5). The $^{206}\text{Pb}/^{204}\text{Pb}$ ratios vary between 19.3 and 20.1.

Our results, in conjunction with data from the literature [1–3], suggest the involvement of three mantle source components (or their mixtures) during the formation of Ross Sea magmas: depleted MORB-type mantle, an enriched mantle component (EM), and a component akin to HIMU. The involvement of these mantle components during magma genesis correlates with tectonic setting: whereas MORB-type compositions are restricted to Recent within-rift basalts, EM and HIMU isotope signatures dominate off-rift magmas from the western rift shoulder and Marie Byrd Land respectively.

Basalts from the western rift shoulder show temporal isotopic and trace element variations from EM towards HIMU-type signatures between 15 and 5 m.y. On the other hand, within-rift and Marie Byrd Land basalts changed from HIMU-type towards MORB-type compositions through time. These temporal geochemical variations together with the respective tectonic settings of magmatism suggest that the mantle beneath the Ross Sea Rift is stratified in the order MORB- to HIMU- to EM-type sources. It appears that during rift evolution the EM- and HIMU-type sources are consumed and depleted asthenospheric MORB-type mantle rises progressively into the melting region. This suggests that EM resides in the mantle lithosphere. The HIMU-type component may be related to the head of

¹ Present address: Mineralogisch–Petrographisches Institut, Universität Heidelberg, Im Neuenheimer Feld 236, D-69120 Heidelberg, Germany

² Present address: Geochemisches Institut, Universität Göttingen, Goldschmidtstrasse 1, D-37077 Göttingen, Germany

an active or, alternatively, ‘fossilized’ mantle plume attached to the base of the lithosphere beneath the Ross Sea area.

1. Introduction

Studies on continental alkali basalts have revealed that many of them have not been contaminated by crust en route to the surface (e.g., [4]) and that their sources are similar to those of OIB with respect to their geochemical and isotopic character (e.g., [5]). Alkali basalts may therefore bear important information on the type and composition of mantle sources beneath the continents. In particular, rift-related alkali basalts may be used to trace the temporal involvement of various magma sources during rift evolution and may, in turn, provide important information regarding the structure of the subcontinental mantle.

The Ross Sea Rift (RSR) represents one of the largest continental rift systems on Earth. The extensive set of geophysical data (e.g., [6–8] and references therein), our knowledge about the structure and tectonic development (e.g., [6–10] and references therein) and the available age information on the uplift (e.g., [11]) and rift-related magmatism (e.g., [12,13]) make this area suitable for studying the relationships between geological, geophysical and geochemical parameters in continental rift systems.

This study documents the Nd, Sr, and Pb isotopic compositions of Cenozoic near-primary to differentiated volcanic rocks of the McMurdo Volcanic Group from several regions along the western margin of the RSR in Northern Victoria Land (NVL). The samples represent different stages in the evolution of the rift, ranging in age between 15 Ma and present and erupted in different tectonic environments. The major aims of the study are (1) to determine the isotopic compositions and types of the mantle sources involved in the petrogenesis of the near-primary basalts, (2) to establish possible relationships between isotopic signature, tectonic setting and rift evolution and (3) to deduce a model for the mantle structure beneath the RSR. We present

our data in combination with published trace element data [14] and data for the basalts from Mt. Melbourne [1] and Marie Byrd Land [2,3].

2. Geological background

The Ross Sea Rift (RSR) represents one of the major active continental extension zones on Earth. Starting at the Antarctic continental margin within the Ross Sea area, the rift extends inland for more than 3000 km, forming a 1000 km wide curved depression filled with thick sequences of predominantly Cenozoic sediments [6]. The topographic rift margins are formed by the Transantarctic Mountain Range (TAM) in the west and Marie Byrd Land (MBL) in the east. However, while the TAM represents a true rift shoulder, MBL does not, the latter instead consisting of a series of rift basins and extended crust, similar to that observed in the Basin and Range province ([8] and Kyle, pers. commun.). In Victoria Land the rift trough is divided into the Eastern, Central and Victoria Land Basins (Fig. 1). The Victoria Land Basin differs from the others by virtue of its drastically greater depth of about 10–14 km (as compared to 5–6 km) [6,9]. Geophysical and geological studies show that its western flank is characterized by a major fault separating the basin from the adjacent 4000 m high TAM rift shoulder, represented by a 3000 km long and 100–200 km wide mountain range which has been gently tilted and block-faulted during vertical uplift [9,11,15]. Gravity and seismic data suggest that the depth of the Moho changes drastically from about 40 km beneath the TAM to about 20 km beneath the Ross Sea Basin, indicating that the crust has been strongly rifted and thinned beneath the Victoria Land Basin [6]. Rifting and lithospheric thinning took place in two major phases: one that was contemporaneous (and related?) with the breakup of Australia–New Zealand and Antarctica (ca. ≥ 90

Ma) resulting in wide sedimentary basins in the Ross Sea, and a second phase during the Cenozoic associated with TAM uplift and the forma-

tion of Terror Rift and its rift-related magmatism (e.g., [9]). Volcanism occurred from > 30 Ma to present ([12,13] and references therein) and is

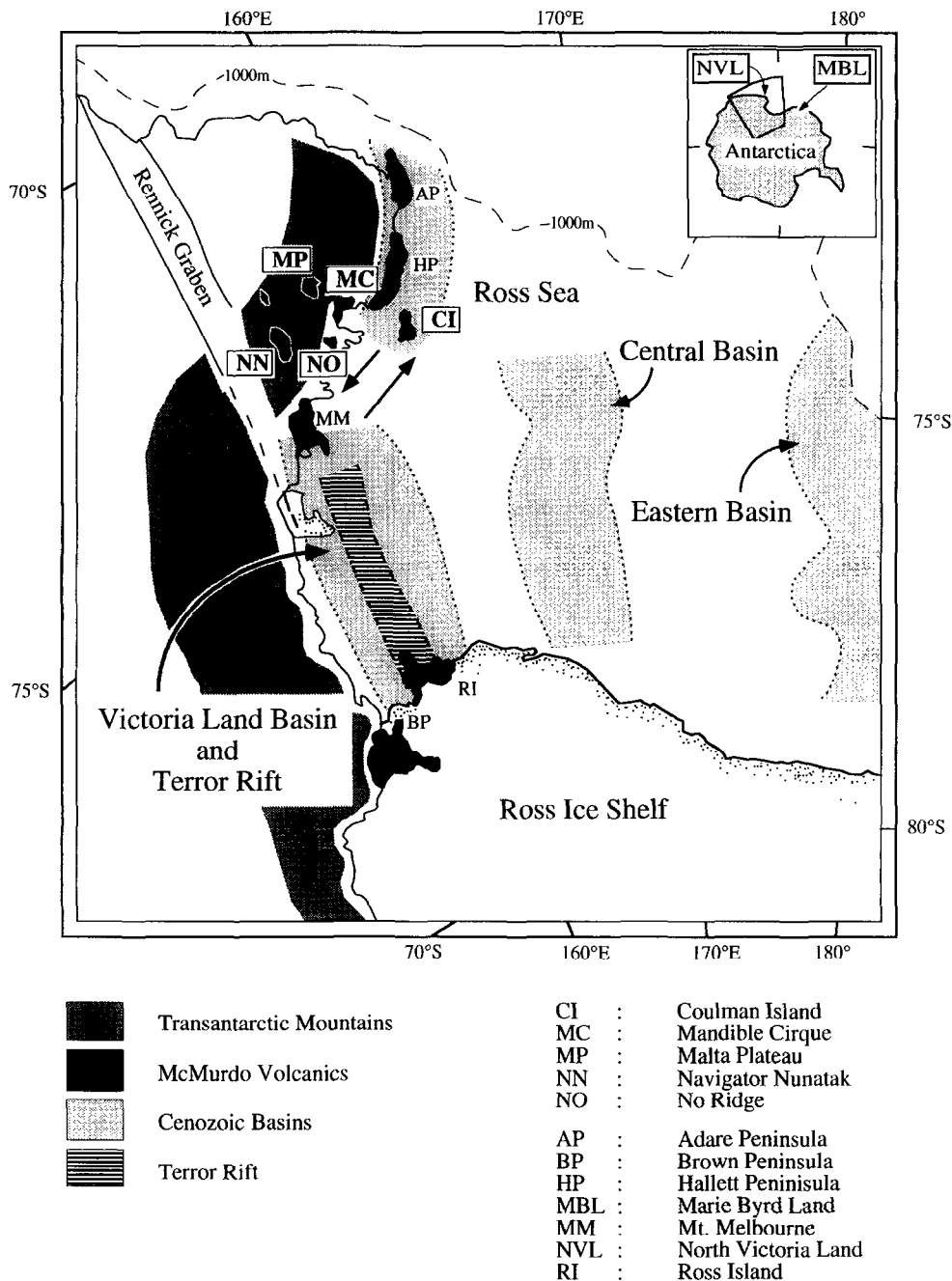


Fig. 1. Simplified structural map of Northern Victoria Land (NVL) and the adjacent Ross Sea margin. Early rift basins (Victoria Land and Central and Eastern Basins) and the younger Terror Rift are after [1,6,7]. McMurdo Volcanics (black) are aligned along the rift margin parallel to the uplifted Transantarctic Mountains (TAM).

Table 1
Sr and Nd isotopes in McMurdo Volcanics

sample	rock type (1)	age (Ma) (2)	remark (3)	$^{87}\text{Sr}/^{86}\text{Sr}_M$ (4)	$^{143}\text{Nd}/^{144}\text{Nd}_M$ (4)	$^{87}\text{Sr}/^{86}\text{Sr}_T$ (5)	$^{143}\text{Nd}/^{144}\text{Nd}_T$ (5)	$\epsilon_{\text{Nd } T}$ (5)	$^{87}\text{Rb}/^{86}\text{Sr}$ (6)	$^{147}\text{Sm}/^{144}\text{Nd}$ (6)
<u>COULMAN ISLAND (within-rift):</u>										
CI-1	BEN	8 ± 2	ml sl	0.702902 ± 16 0.702918 ± 16	0.512934 ± 13 0.512942 ± 7	0.702874 ± 24	0.512929 ± 14	5.9	0.250	0.095
CI-103	AB	8 ± 2	ml sl	0.702828 ± 17 0.702938 ± 44	0.512917 ± 14 0.512854 ± 40	0.702814 ± 21	0.512911 ± 16	5.5	0.128	0.113
CI-303	HAW	8 ± 2	ml sl l	0.703239 ± 17 0.703262 ± 15 0.703392 ± 20	0.512878 ± 4 0.512881 ± 21	0.703207 ± 26	0.512872 ± 6	4.8	0.285	0.112
<u>MALTA PLATEAU (western rift shoulder):</u>										
MA-6	TRAB	15 ± 2	ml sl	0.703537 ± 7 0.703441 ± 9	0.512802 ± 13 0.512811 ± 3	0.703487 ± 15	0.512791 ± 15 (8)	3.4 (8)	0.246	-
MA-9	AOB	15 ± 2	ml sl	0.705069 ± 20 0.705243 ± 81	0.512698 ± 6 0.512689 ± 11	0.705041 ± 24	0.512686 ± 8	1.3	0.130	0.128
MA-100	RHY	15 ± 2	ml sl	0.734629 ± 20 0.736339 ± 17	0.512791 ± 13 0.512788 ± 6	0.704167 ± 4700	0.512779 ± 15	3.1	143	0.128
MA-117	AOB	15 ± 2	ml sl	0.703819 ± 16 0.703777 ± 17	0.512802 ± 14 0.512824 ± 10	0.703786 ± 21	0.512789 ± 16	3.3	0.162	0.134
MS-3412	RHY	15 ± 2	ml	0.712179 ± 15	0.512664 ± 14	0.704084 ± 1260	0.512651 ± 16 (8)	0.6 (8)	38.0	-
<u>MANDIBLE CIRQUE (transitional):</u>										
MS-3387	HAW	7 ± 3	ml sl l	0.703784 ± 16 0.703783 ± 10 0.703861 ± 15	0.512869 ± 5 0.512870 ± 20 0.512855 ± 6	0.703767 ± 24	0.512864 ± 7	4.6	0.170	0.113
<u>NAVIGATOR NUNATAK & LOCAL SUITE (western rift shoulder):</u>										
NN-10	BAS	5 ± 3	ml sl l	0.703211 ± 13 0.703219 ± 10 0.703304 ± 21	0.512883 ± 20 0.512891 ± 10 0.512894 ± 12	0.703193 ± 24	0.512879 ± 22	4.8	0.254	0.108
SC-2	MUG	5 ± 3	ml sl	0.703353 ± 20 0.703359 ± 30	0.512895 ± 15 0.512912 ± 20	0.703339 ± 28	0.512892 ± 17	5.1	0.194	0.103
<u>NO RIDGE (western rift shoulder):</u>										
NO-5	AB	10 ± 10 (7)	ml sl	0.703171 ± 15 0.703236 ± 21	0.512903 ± 12 0.512921 ± 28	0.703155 ± 31	0.512895 ± 20 (8)	5.3 (8)	0.111	-
NBS 987				0.710231 ± 8 (9)	-					
La Jolla				-	0.511825 ± 6 (10)					

(1) AB = alkali basalt; BAS = basanite; MUG = mugearite; TRAB = trachybasalt; HAW = hawaiiite; AOB = alkali olivine basalt; BEN = benmoreite; RHY = rhyolite; TRA = trachyte.

(2) Assumed average K-Ar ages for respective volcanic fields after [12].

(3) ml = mildly leached; sl = strongly leached; l = leachate.

(4) M = measured values, fractionation corrected with $^{86}\text{Sr}/^{88}\text{Sr} = 0.1194$ and $^{146}\text{Nd}/^{144}\text{Nd} = 0.7129$; in-run errors are 2σ of the mean.

(5) T = initial values, calculated by using Rb-Sr and Sm-Nd concentrations from [14]; error propagation includes analytical and age uncertainties.

(6) Atomic ratios calculated from Table 2.

(7) Estimated age assuming that 25 Ma old Meander intrusives at No Ridge locality [12] are older than capping McMurdo Volcanics.

(8) Because of missing Sm-Nd concentrations, $^{143}\text{Nd}/^{144}\text{Nd}_T$ and $\epsilon_{\text{Nd}(t)}$ were calculated by assuming typical Sm/Nd ratios.

(9) and (10) Between-run precision (2σ of the mean) based on 43 measurements of NBS 987 and 28 measurements of La Jolla standards.

Table 2
Major (%) and minor elements (ppm) from [14]

	CI-1	CI-103	CI-303	NN-10	SC-2	NO-5	MA-6	MA-9	MA-100	MA-117	MS-3412	MS-3387
SiO ₂	56.09	45.08	50.45	40.90	48.56	45.29	49.55	48.75	72.11	46.84	76.18	47.87
TiO ₂	1.02	3.28	2.57	2.42	2.97	2.45	2.48	2.39	0.32	2.62	0.09	2.74
Al ₂ O ₃	19.06	16.77	16.66	11.46	16.32	19.32	15.69	13.92	10.15	14.19	12.23	15.60
Fe ₂ O ₃	3.57	8.21	6.14	3.84	3.78	5.54	3.42	2.68	2.00	3.50	1.34	10.34
FeO	2.81	3.71	3.22	7.11	6.53	4.10	7.25	8.48	3.16	8.28	0.05	3.02
MnO	0.25	0.20	0.21	0.21	0.18	0.15	0.19	0.16	0.13	0.19	0.02	0.24
MgO	0.92	4.33	2.82	11.18	4.26	2.99	3.37	9.14	0.04	8.38	0.05	3.10
CaO	4.06	9.91	7.03	9.87	7.46	9.48	6.79	9.73	0.32	10.83	0.30	7.62
Na ₂ O	6.89	3.00	3.87	2.53	4.52	3.38	4.09	2.18	5.06	2.62	3.37	4.07
K ₂ O	2.88	1.67	2.52	1.88	2.39	1.48	2.23	0.87	4.54	1.14	4.69	1.87
P ₂ O ₅	0.24	0.75	0.97	0.78	0.94	0.63	1.28	0.31	0.01	0.42	0.01	1.51
L.O.I.	0.89	2.06	1.82	5.96	0.54	3.85	2.45	0.82	0.87	0.44	0.73	0.89
total	98.68	98.97	98.28	98.14	98.45	98.66	98.79	99.43	98.71	99.45	99.06	98.87
Mg-value	24	44	40	68	47	40	40	63	-	60	-	34
Mg#	37	68	61	74	54	57	45	66	-	64	-	65
Ba	806	404	656	705	620	254	565	229	8	337	77	603
Y	45	35	48	40	22	31	51	24	119	33	42	47
Sr	1052	826	711	890	1078	928	803	461	5	531	18	789
Rb	92	37	71	79	73	36	69	21	250	30	239	47
Zn	113	121	124	147	123	101	153	108	201	108	74	143
Cu	6	18	9	58	44	40	13	22	6	42	3	11
Co	44	50	28	53	75	35	26	70	27	57	72	36
Cr	1	12	9	426	64	9	1	272	1	349	1	1
V	16	259	145	188	139	151	109	254	6	302	1	107
Nb	206	87	114	133	126	44	83	28	257	52	83	102
Zr	653	310	409	465	617	217	440	172	1500	200	159	362
Ni	2	10	5	200	34	13	4	86	1	93	1	5
La	103	51.6	69.3	84.2	90.0	n.d.	n.d.	24.4	172	32.7	n.d.	69.8
Ce	200	106	145	156	178	n.d.	n.d.	50.9	326	66.8	n.d.	147
Pr	21.0	12.5	17.3	16.9	20.1	n.d.	n.d.	6.39	36.5	8.00	n.d.	17.2
Nd	71.2	52.3	67.2	62.2	74.8	n.d.	n.d.	25.9	129	32.0	n.d.	71.9
Sm	11.2	9.76	12.5	11.1	12.8	n.d.	n.d.	5.47	27.3	7.08	n.d.	13.5
Eu	3.53	3.10	3.58	3.27	3.99	n.d.	n.d.	1.77	0.92	2.13	n.d.	4.27
Gd	8.99	8.70	10.3	8.80	10.8	n.d.	n.d.	5.09	23.3	6.76	n.d.	11.7
Tb	1.28	1.25	1.53	1.23	1.47	n.d.	n.d.	0.82	3.76	1.00	n.d.	1.46
Dy	8.52	7.62	8.73	6.51	8.15	n.d.	n.d.	4.54	22.0	5.67	n.d.	8.60
Ho	1.69	1.34	1.64	1.17	1.64	n.d.	n.d.	0.80	4.33	1.10	n.d.	1.53
Er	4.49	3.41	4.33	2.99	4.57	n.d.	n.d.	2.07	11.35	3.06	n.d.	3.89
Tm	0.72	0.49	0.59	0.40	0.67	n.d.	n.d.	0.29	1.70	0.40	n.d.	0.49
Yb	4.67	2.97	3.59	2.43	3.81	n.d.	n.d.	1.73	11.0	2.55	n.d.	3.09
Lu	0.73	0.66	0.50	0.32	0.52	n.d.	n.d.	0.37	1.59	0.37	n.d.	0.44

Mg value = 100MgO/(MgO + 0.85 * FeO_{tot}). Mg# = 100Mg/(Mg + Fe²⁺). L.O.I. = loss on ignition. n.d. = not determined.

related to basin subsidence and TAM uplift [6,9,16]. MBL is interpreted as a microplate attached to the Antarctic continent during the Paleozoic [17]. The lack of a scarp fault between the RSR and MBL (as observed in the TAM) and the markedly different crustal thicknesses at MBL (≈ 32 km) and at TAM (≥ 40 km) highlights the asymmetric structure of the rift (e.g., [8,9]).

Rift-related volcanic rocks along the western rift margin belong to the Cenozoic McMurdo Volcanic Group, which comprises the Mt. Melbourne and Hallett Volcanic Provinces in Northern Victoria Land (NVL) and the Erebus Province in Southern Victoria Land ([18] and references therein). Occurrences of each province include both within-rift and TAM shoulder locations. Recently, Behrendt et al. [8] and Hole and LeMasurier [3] have argued for a plume-related origin for the RSR (which they call the 'West Antarctic Rift System') with a (HIMU-) plume centred beneath the MBL volcanic province.

Primitive basaltic McMurdo magmas include both alkali basalts and basanites. Few of these rocks meet the criteria for primary magmas (i.e., $100\text{Mg}/(\text{Mg} + \text{Fe}^{2+}) \geq 68$ and $\text{Ni} \geq 320$ ppm [18]), indicating that some olivine + clinopyroxene fractionation has occurred. These rocks are therefore classified as near-primary [14]. Compared to alkali basalts, basanites are generally more primitive and significantly enriched in incompatible trace elements [14]. The basanites commonly contain abundant mantle and lower crustal xenoliths [20], which are absent in alkali basalts. Differentiated rocks derived from alkali basaltic magmas include trachybasalts, rhyolites and alkali syenites [14].

3. Samples and analytical techniques

The samples studied include rocks from the Hallett (Coulman Island and Mandible Cirque) and Melbourne Provinces (Fig. 1). In structural terms the samples represent rocks erupted within the Victoria Land Basin (Coulman Island), off-rift rocks erupted on the western rift shoulder of the TAM (Malta Plateau and Navigator Nunatak) and rocks erupted transitionally (i.e., between the

two other structural units) (Mandible Cirque). Refer to Fig. 1 and Table 1 for further details. Precise sample localities are given in [14]. The rock types include near-primary basalts (alkali basalts and basanites) and differentiated rocks including trachybasalts and rhyolites (Table 1). The major and trace element compositions [14] are listed in Table 2.

Chemical extraction of Sr and Nd for mass spectrometry followed White and Patchett [21]. Total procedure blanks were about 60 pg for Nd and 100 pg for Sr. Sr and Nd isotope analyses were carried out on Finnigan MAT 261 mass spectrometers at the *Max-Planck-Institut* in Mainz. Pb analyses were carried out at Woods Hole Oceanographic Institution. The chemical procedures followed Taras and Hart [22]. The Pb blanks ranged between 25 and 75 pg. Mass spectrometric analyses were carried out statically with five collectors.

In order to remove possible surface alteration effects and seaspray deposits all the sample powders were gently washed in warm 0.5N HCl for about 15 min before analysis. In addition, other splits of the same rock powders were strongly leached with hot 6N HCl for several hours. Mildly and strongly leached samples of ≤ 8 Ma old basaltic rocks yielded, within error, identical Sr and Nd isotopic compositions (although CI-103 is an exception). This suggests that the Nd and Sr systematics of these samples were not disturbed by surface alteration. Minor but insignificant differences exist in ≥ 15 Ma old basaltic rocks from Malta Plateau and may be partly due to in-situ growth of radiogenic ^{87}Sr and/or to contamination by surface alteration and/or seaspray. In contrast to basaltic rocks, large Sr isotopic differences between mildly and strongly leached powder aliquots exist for the highly evolved rocks (e.g., rhyolite MA-100). In the following discussion and diagrams we only use initial values from the mildly leached whole-rock samples.

4. Results

The measured and initial Nd and Sr isotope data are listed in Table 1. The initial isotope

ratios were calculated using published K-Ar ages [12] and Rb-Sr and Sm-Nd concentrations [14]. Where precise K-Ar ages are unknown, we assumed an average age for the respective volcanic region. Differences between measured and initial $^{87}\text{Sr}/^{86}\text{Sr}$ ratios are insignificant for basaltic rocks but are large for strongly fractionated high-Rb/Sr rocks such as rhyolite MA-100. Because the uncertainty in the assumed age for the latter results in large isotopic uncertainties, these rocks are not considered in our interpretation. On the other hand, measured and initial $^{143}\text{Nd}/^{144}\text{Nd}$ ratios are indistinguishable within error for all rocks. The measured Pb isotopes are listed in Table 3.

Table 3
Pb isotope ratios in McMurdo Volcanics

	$^{206}\text{Pb}/^{204}\text{Pb}$	$^{207}\text{Pb}/^{204}\text{Pb}$	$^{208}\text{Pb}/^{204}\text{Pb}$
CI-103	20.143	15.663	39.600
CI-303	19.472	15.617	39.324
MA-117	19.320	15.620	39.270
NN-10	19.996	15.611	39.741
SC-2	19.902	15.612	39.416
NO-5	19.703	15.577	39.387

Isotope ratios corrected to values given in [50] for Pb standard NBS 981. In-run errors (2σ) are 0.01% or less. Reproducibility or between-run precision is typically 0.04%/amu. Isotope ratios are corrected for 0.05–0.1% fractionation/amu.

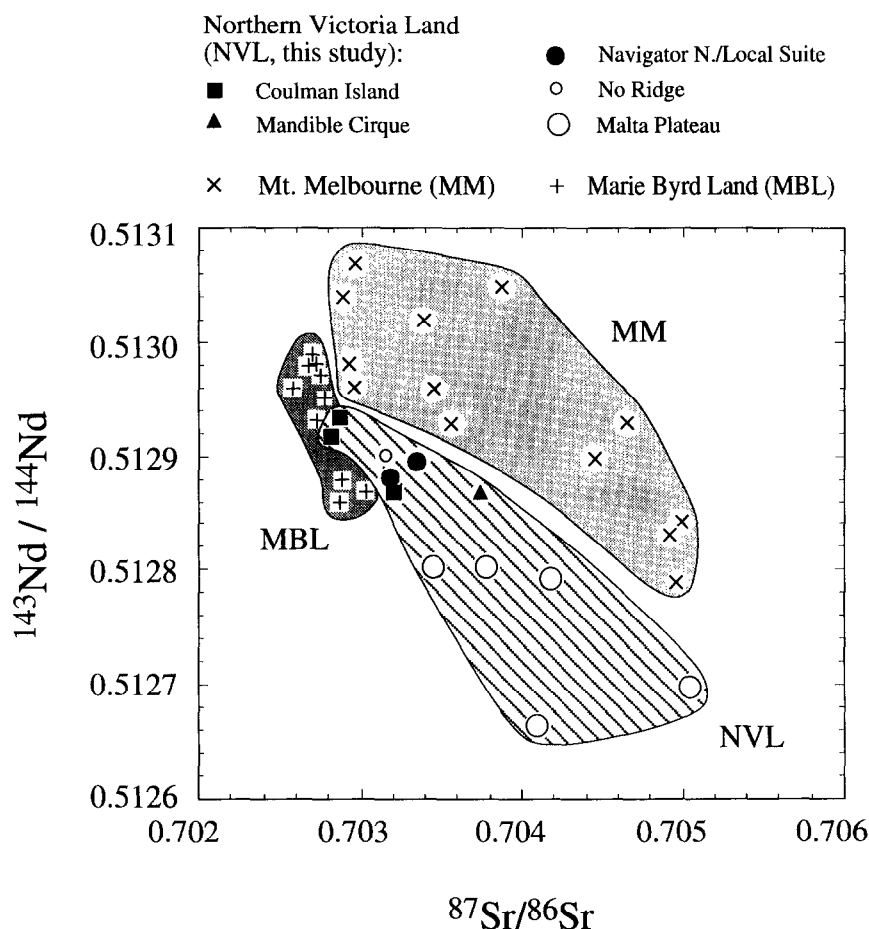


Fig. 2. $^{87}\text{Sr}/^{86}\text{Sr}$ and $^{143}\text{Nd}/^{144}\text{Nd}$ initial isotopic ratios for McMurdo Volcanics from Northern Victoria Land (NVL, this study). Reference fields for Mt. Melbourne volcanics (MM) from [1] and for Marie Byrd Land (MBL) from [2,3].

The NVL rocks show significant variations in initial Sr and Nd isotopic ratios (Table 1). The complete range in $^{87}\text{Sr}/^{86}\text{Sr}$ and nearly the complete range in $^{143}\text{Nd}/^{144}\text{Nd}$ is covered by the alkali basalts alone (Table 1). Sr isotope values vary between 0.70281 (alkali basalt CI-103) and 0.70504 (alkali olivine basalt MA-9). The Nd isotope ratios range from 0.51269 (alkali olivine basalt MA-9) to 0.51293 (benmoreite CI-1) and the $\epsilon_{\text{Nd}(t)}$ values range from +1.3 to +5.9. The Pb isotope ratios range from $^{206}\text{Pb}/^{204}\text{Pb} = 19.32$ to 20.14, from $^{207}\text{Pb}/^{204}\text{Pb} = 15.58$ to 15.66, and from $^{208}\text{Pb}/^{204}\text{Pb} = 39.27$ to 39.60 (note that MA-9 has not been analyzed for Pb).

In Fig. 2 the initial Nd and Sr isotope ratios of the NVL samples (grouped according to their

geographical location) are compared to published data from Mt. Melbourne Province [1] and MBL [2,3]. NVL rocks show a very wide range with respect to initial Sr and Nd isotopes, enlarging considerably the isotope range for Ross Sea volcanics towards more 'enriched' values. The depleted range for NVL rocks overlaps slightly with the field for MBL alkali basalts, whereas no overlap exists with rocks from Mt. Melbourne. We note that each NVL field can be characterized by a specific isotopic signature with only a limited overlap in Nd-Sr isotope space.

In terms of mantle component end members [23,24] our rocks form a quasi-linear negative correlation trend in Sr-Nd isotope space, within a triangle formed by depleted MORB-type mantle

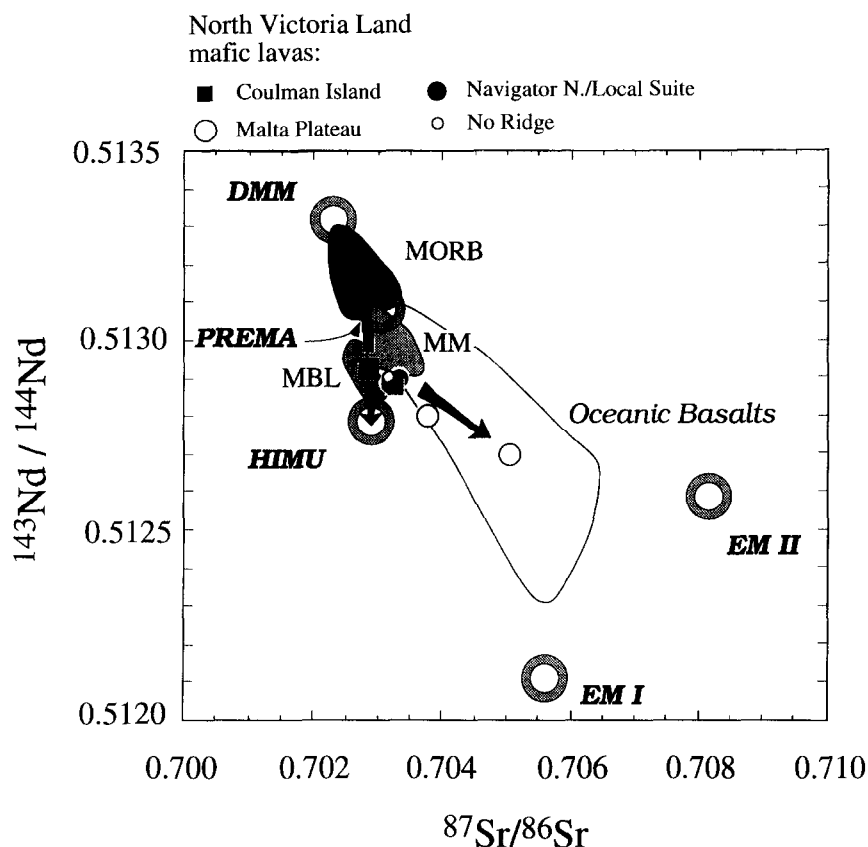


Fig. 3. $^{87}\text{Sr}/^{86}\text{Sr}$ and $^{143}\text{Nd}/^{144}\text{Nd}$ initial isotopic ratios for mafic McMurdo Volcanics from NVL. Reference fields for MM and MBL mafic volcanics after [1–3]. Reference fields for mantle components after [23,24]. NVL rocks plot along a negative correlation trend within a triangle defined by depleted mantle (DMM or PREMA), HIMU and enriched mantle of hybrid composition between EM I and EM II.

(DMM or PREMA), a HIMU-like component and an enriched component hybrid between EMI and EMII (Fig. 3).

5. Mantle source variations versus crustal assimilation

The question of whether a suite of basalts has been contaminated by continental crust is critical to the evaluation of their source characteristics. This problem is especially serious for basalts displaying EM-type signatures, because both an origin from enriched mantle sources and assimilation of continental crust by basaltic magmas may yield similar mixing arrays in Nd-Sr isotope diagrams. Two of the analyzed near-primary basalts (MA-9 and MA-117) show enriched isotope sig-

natures and might therefore be suspected of being contaminated by continental crust.

We see manifold geochemical evidence that these samples have not been contaminated by continental crust. For example, the high Mg# (> 64) and Ni contents (≈ 90 ppm) cannot be reconciled with the extraordinary high degrees of AFC-type contamination required from Sr-Nd isotope mass calculations (10% for average upper crust and > 35% for average lower crust [25]). The REE patterns of the two samples [14] are parallel and the lack Eu anomalies expected for assimilation of crustal material. Furthermore, the ratios between many trace elements are identical in the isotopically most enriched sample (MA-9) and the isotopically most depleted and unequivocally not contaminated alkali basalt (CI-103) but are very different from crustal values [25]. For

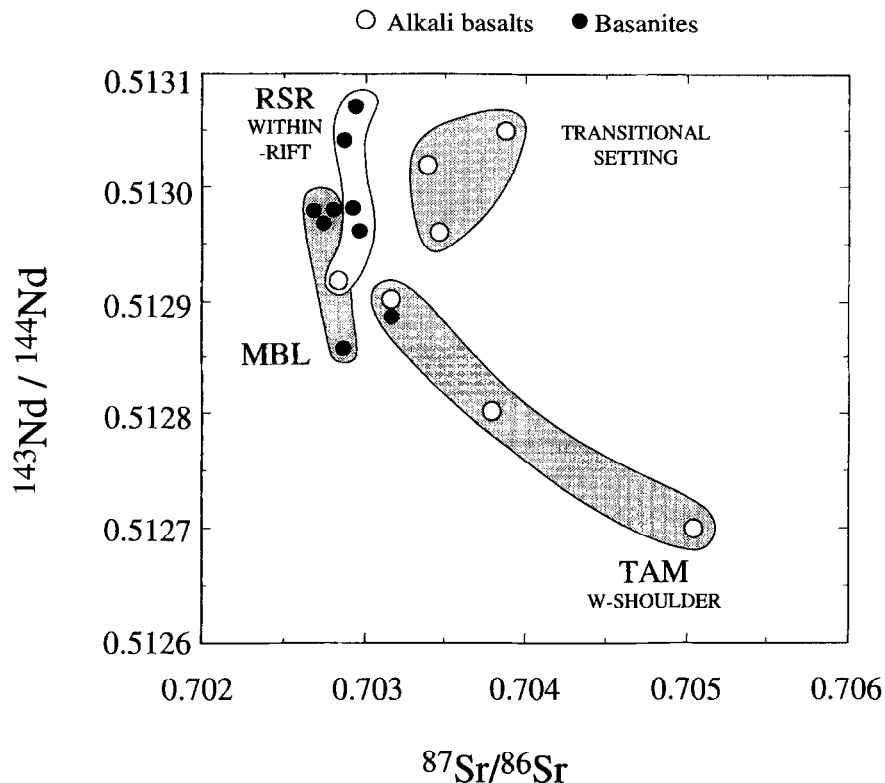


Fig. 4. $^{87}\text{Sr}/^{86}\text{Sr}$ and $^{143}\text{Nd}/^{144}\text{Nd}$ initial isotopic ratios for near-primary basalts from NVL (this study), MM [1] and MBL [2,3] grouped according to relative setting with respect to the rift structure. Rocks from the western rift shoulder (TAM), MBL, within-rift and transitional settings show distinct isotopic variations suggesting binary mixing between different mantle sources.

instance, both samples have ‘oceanic island-type’ Ba/Rb ratios of about 11 (in contrast to Ba/Rb = 5 and 28 in average upper and lower crust respectively), Sr/Rb = 22 (in contrast to 3 and 43), and Zr/Sm = 31 (compared to 42 and 22). The Ba/Nb ratios, which range between 20 and 150 in various crustal reservoirs [25,26], are very low and constant (4–8) in all the near-primary basalts of this study (i.e., they are similar to those displayed by various types of oceanic basalts (e.g., [27])). Moreover, this ratio correlates positively with Mg# (not shown), which is the opposite to what would be expected for assimilation. In diagrams involving trace element and isotope covariations (such as Zr/Nb versus $^{143}\text{Nd}/^{144}\text{Nd}$ or $^{87}\text{Sr}/^{86}\text{Sr}$ (not shown)) the variations for near-primary magmas trend away from mixing arrays between primitive magmas and crustal end members. These observations preclude any substantial degree of crustal assimilation for modifying effectively the Nd and Sr isotopes of primitive magmas. We conclude that the near-primary basalts from NVL, including those with EM-type signatures, show no effects of contamination by continental crust and may therefore be used to constrain the Sr and Nd isotopic composition of their mantle sources.

6. Isotope and trace element variations in space and time

6.1. Structural control

It has been pointed out that (a) volcanic rocks from NVL show a very wide range in initial Sr and Nd isotopes, (b) each volcanic field is characterized by a specific Nd-Sr signature and (c) little or no overlap exists with rocks from the Mt. Melbourne province and MBL (Fig. 2). The question arises as to whether these differences between magmas from different localities are independent features or whether they are coupled with geological processes relating to the evolution of the rift.

Fig. 4 discriminates between near-primary basalts erupted (a) within the RSR, (b) on the TAM shoulder, (c) transitionally between rift and the TAM shoulder, and (d) in MBL. In this

diagram, magmas from different structural settings occupy individual fields with no or little overlap. For instance, Sr and Nd isotopes in TAM shoulder basalts have relatively enriched isotope values and correlate inversely over a wide range of isotopic compositions ($^{87}\text{Sr}/^{86}\text{Sr} \approx 0.7031\text{--}0.7050$, $^{143}\text{Nd}/^{144}\text{Nd} \approx 0.51269\text{--}0.51290$, $\epsilon_{\text{Nd}(t)} \approx 1.3\text{--}5.3$). The isotopically most enriched sample is alkali basalt MA-9. In contrast, basanites from MBL show a very limited range in $^{87}\text{Sr}/^{86}\text{Sr}$ (from about 0.7027 to 0.7029) and only moderate variations in $^{143}\text{Nd}/^{144}\text{Nd}$ (from 0.51285 to 0.51298, $\epsilon_{\text{Nd}(t)} = 4.5\text{--}6.7$). Within-rift rocks form a steep trend which is characterized by nearly uniform $^{87}\text{Sr}/^{86}\text{Sr}$ ratios ($\approx 0.7028\text{--}0.7030$) and $^{143}\text{Nd}/^{144}\text{Nd}$ ratios ranging between about 0.51291 and 0.51307 (i.e., $\epsilon_{\text{Nd}(t)} \approx 5.5\text{--}7.9$). The enriched side of this trend lies between values for rocks from MBL and the TAM shoulder, whereas the depleted side of the trend falls within the MORB field (Fig. 3).

In isotopic respects, transitional rocks from the Mt. Melbourne and Mandible Cirque localities (i.e., rocks which erupted between the Victoria Land Basin and the TAM shoulder) fail to show their isotopically transitional character. Instead, they plot in a separate field subparallel to the main trend showing no overlap with rocks from the TAM shoulder or within-rift localities.

Our Sr-Nd data fall in a triangle defined by depleted MORB-type mantle (DMM or PREMA), a HIMU-like component and an enriched component hybrid between EMI and EMII [23,24] (Fig. 3). Under the assumption that intermediate isotope compositions represent mixtures of extremes, these three source components (or their mixtures) appear to be involved in the genesis of the RSR magmas. In this scenario the elongate, narrow fields for MBL, within-rift and TAM shoulder basalts represent binary mixing lines. The steep array in the Sr-Nd isotope correlation diagram for within-rift basalts is derived from slightly different proportions of depleted MORB-type mantle and a HIMU-like component characterized by low $^{87}\text{Sr}/^{86}\text{Sr}$ and intermediate $^{143}\text{Nd}/^{144}\text{Nd}$ ratios. It seems very likely that the latter component itself represents a mixture between HIMU and PREMA-like depleted mantle.

Basanites from MBL follow a mixing trend sub-parallel to that formed by the within-rift basalts. This trend indicates a stronger contribution by

HIMU. A third component is indicated by mafic lavas from the TAM shoulder which tend to have more radiogenic $^{87}\text{Sr}/^{86}\text{Sr}$ ratios. This may record

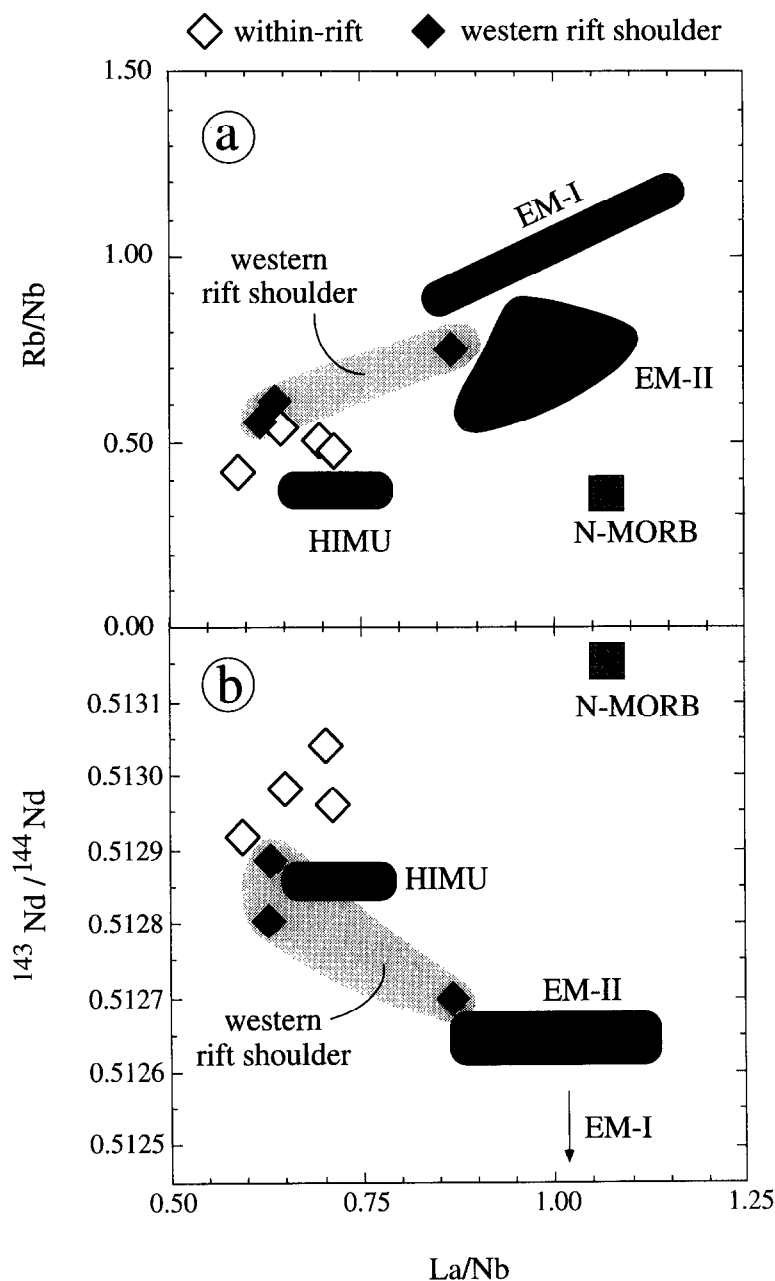


Fig. 5. La/Nb versus Rb/Nb (a) and initial $^{143}\text{Nd}/^{144}\text{Nd}$ ratios (b) in near-primary basalts from the Ross Sea Rift (RSR) erupted in different structural settings. Trace element data after [1,14]. Reference fields for mantle components after [23,24,27]. While the HIMU component is visible both in within-rift and rift shoulder rocks, the involvement of enriched mantle is only reflected in rocks from the western rift shoulder.

the involvement of an EM-type mantle component hybrid between EMI and EMII. The presence of MORB-type, HIMU-type and enriched signatures in magmas from the western RSR has also been observed by Hart and Kyle [28]. These authors argue that the Sr-enriched signature of the TAM magmas was caused by crustal assimilation during ascent through thick TAM crust, compared to thin crust beneath the within-rift localities. However, our interpretation, in contrast, is based both on isotopic and trace element evidence and we argue against contamination and for an enriched mantle source component (Section 5.1).

The presence of HIMU-type mantle beneath NVL is supported by Pb isotope data (Table 3). The highly radiogenic Pb isotopes indicative of this component are found both in within-rift and TAM rocks. HIMU-dominated Pb isotopes have also been reported from various other RSR localities, including Ross Island [4], MBL and the Balleny Islands [28–30]. Obviously, HIMU-type mantle is a very common phenomenon throughout the northern RSR [28,30]. Note that the Pb

isotopes of EM-dominated basalt MA-117 are very similar to EMI oceanic basalts [29].

It was pointed out that volcanic rocks which erupted in a tectonically transitional position fail to show their transitional character with respect to their isotopic composition. One plausible explanation invokes the involvement of an additional enriched component with distinct trace element and isotope characteristics resulting in mixing lines that differ from those observed for TAM shoulder rocks.

None of the recognized mantle components has the highly enriched isotopic (and chemical) signature which has been proposed for the origin of the Jurassic Ferrar large igneous province exposed along the TAM [31]. This either suggests that sediment-subduction-modified mantle [31] was not tapped during RSR magmatism or that crustal contamination has caused the unusual trace element and isotopic signature of the Ferrar rocks.

We summarize by stating that the Nd, Sr and Pb isotopic variations in primitive basalts from the RSR reflect marked isotopic differences be-

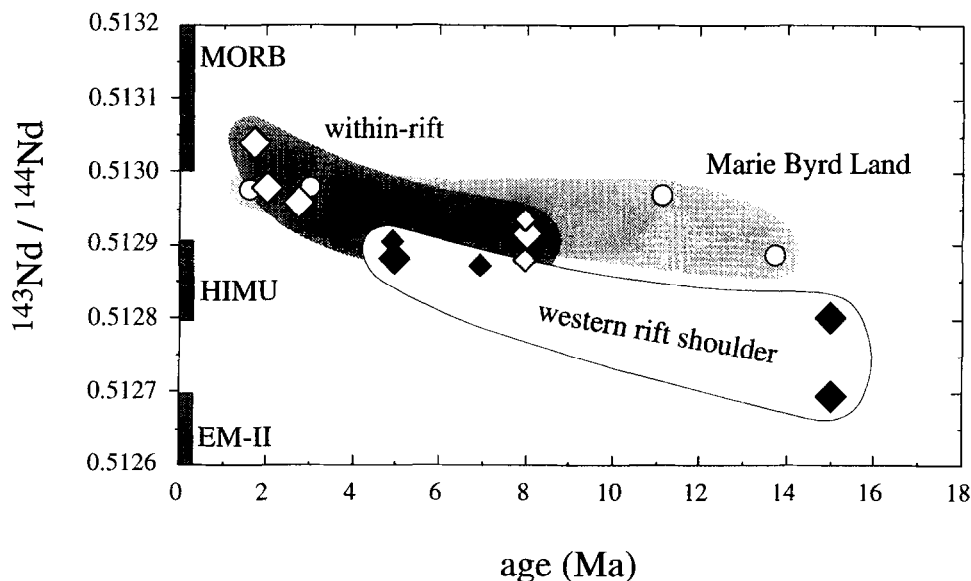


Fig. 6. Temporal variation in initial Nd isotopes in Ross Sea basalts. Western rift shoulder (\blacklozenge) and within-rift basalts (\blacklozenge) evolved towards more depleted compositions through time, reflecting a change in mantle sources during rift evolution. Basanites from MBL (\circ) [2,3] show only a slight increase in $^{143}\text{Nd}/^{144}\text{Nd}$ from 14 Ma onwards. Large symbols = alkali basalts and basanites; small symbols = differentiated basalts. Age data from [2,3,12].

tween basalts erupted in different rift-related tectonic environments and indicate the presence of three mantle components (MORB-, EM- and HIMU-type mantle) beneath Northern Victoria Land.

6.2. Correlations between trace element and isotope ratios

Various authors (e.g., [27,32]) have shown that ratios between highly incompatible elements in OIB reflect those of their sources and may be used to discriminate between the OIB end members. Using these criteria we find HIMU and EM trace element characteristics (Table 2) in Ross Sea magmas with HIMU and EM signatures in their Nd-Sr isotopes. This may be shown by means of the La/Nb ratio, which is often used as an indicator of the mantle sources of basalts (e.g., [27,32–34]). Fig. 5 shows the available data for Ross Sea near-primary basalts in La/Nb versus Rb/Nb (a) and $^{143}\text{Nd}/^{144}\text{Nd}$ (b) diagrams and compares this data to estimates for depleted (N-MORB), HIMU and EM mantle [23,24,27]. In both diagrams basalts from the western rift shoulder reflect a transition from HIMU to EM-type sources, which is in accordance with the observed Sr-Pb isotope values. In contrast, both the La/Nb and Rb/Nb ratios in within-rift basalts are dominated by HIMU-like compositions and, in addition, indicate a trend from HIMU towards MORB-type signatures. These observations show that characteristic trace element ratios are consistent with isotope variations and support the interpretation of three distinct mantle sources being involved in the genesis of the RSR basalts. In particular these relationships are compatible with the existence of HIMU- and EM-like components beneath the western Ross Sea area.

6.3. Temporal isotopic variations as indicators of rift evolution

Fig. 6 displays the initial Nd isotopic compositions of the Ross Sea volcanics versus their eruption ages. This diagram demonstrates that Nd isotopic variations monitor the rift evolution and the successive involvement of various mantle

sources through time. (The same observation holds for Sr isotopes, although the diagram for this is not shown.) For both within-rift and for the western shoulder rocks the magmas evolved towards more depleted signatures with time. On the basis of Fig. 6 and Figs. 2–5 we conclude that the within-rift rocks changed from a HIMU-type at 8 Ma towards more depleted MORB-type signatures today and that rocks from the western rift shoulder changed from EM to HIMU-type signatures between 15 and 5 Ma. Relative to the large isotopic variations observed in the within-rift and western shoulder rocks, basanites from MBL display almost uniform HIMU-type compositions throughout the past 14 Ma. In detail, however, these rocks show a slight increase in $^{143}\text{Nd}/^{144}\text{Nd}$ ratios from 0.51286 to 0.51298, thus reflecting a change from HIMU-type to more depleted mantle sources. This observation has already been pointed out by Futa and LeMasurier [2], who suggest a gradual change from continental or oceanic-island-type sources to a MORB-type source for both primitive and differentiated MBL basalts. We conclude that the observed temporal changes record the consumption of relatively enriched mantle reservoirs and their replacement by more depleted reservoirs with time.

7. Discussion: Mantle structure and rift evolution in the Ross Sea Rift

In the foregoing we have described the temporal and spatial variations in the mantle sources of the RSR basalts. One plausible interpretation for these variations between within-rift, TAM shoulder and MBL magma sources includes lateral isotopic heterogeneities in the lithospheric mantle beneath the RSR. In such a case the lithospheric mantle underlying the TAM and MBL would be dominated by EM- and HIMU-type signatures respectively. This view is compatible with MBL being a microplate attached to the Antarctic continent during the Paleozoic (e.g., [17]). It appears reasonable that the lithospheric mantle sources beneath these two different geological terrains could have developed different isotopic characteristics which were inherited by

the magmas. However, we believe that the ubiquity of HIMU signatures throughout the Ross Sea area [28,30], the structural context of the mantle sources below the rift as indicated by temporal isotopic variations, and indications of a plume origin of the HIMU component (as discussed below) require a more complex model.

It is evident from Fig. 4 that the mixing trends of both the within-rift and TAM shoulder magmas have one end member in common—the HIMU-type component. This observation and the replacement of EM by a HIMU-type source and of HIMU by more depleted mantle sources during rifting (Fig. 6) suggests that during progressive rifting by lithospheric stretching and mantle upwelling the asthenospheric mantle was progressively involved in basalt genesis, thus reducing the influence of HIMU and EM-type components with time. This explains why the most depleted magmas are found in the Victoria Land Basin (i.e., a locality where rifting has progressed furthest and the asthenosphere is essentially at the base of the crust [6]). (Of all the within-rift basalts studied, only hawaiite CI-303 reflects a slight EM influence in its Sr-Nd-Pb isotopic composition.)

Because of its restriction to TAM shoulder localities and its progressive consumption during rifting, the EM component is likely to reside in the mantle lithosphere. This view would accord with observations from mantle xenoliths and continental magmas worldwide, which suggest that enriched signatures are typical features of subcontinental lithospheric mantle (e.g., [35–37]). Furthermore, it has been suggested for the Basin and Range province that the involvement of lithospheric mantle in magma genesis is greatest in regions of maximum lithospheric extension [34]. Recent geophysical models indicate that lithospheric stretching is concentrated beneath the uplifted TAM range [10], which would support a lithospheric origin for EM signatures in TAM magmas.

The progressive replacement of EM-type by HIMU-type sources (TAM shoulder) and of HIMU-type by MORB-type mantle sources (within-rift setting and MBL) can be explained if the mantle beneath the RSR was originally stratified with a HIMU-type source occupying an in-

termediate position between depleted asthenospheric MORB mantle below and enriched lithospheric mantle above. Such chemically and isotopically layered continental lithosphere (EM or HIMU) was also envisaged by Menzies for various continental areas [36,37].

The model presented is in accordance with concepts proposed for other continental rift provinces. For example, Perry et al. [38] noted the correlation of isotopic composition with tectonic setting and various tectomagmatic provinces in the Rio Grande Rift–Basin and Range rift system. These authors suggest that rifting involved thermal thinning and physical replacement of EM-type lithospheric mantle by upwelling-depleted asthenospheric mantle. It is a matter of controversy whether the progressive erosion of the lithospheric mantle beneath this area is caused by lithospheric extension or by thermal erosion by an active mantle plume [33,34,39,40]. Interaction of a HIMU-type plume with depleted asthenospheric and EM-type lithospheric mantle has also been reported from the Canary Islands [41], reflecting comparable replacement trends also in oceanic settings. A progressive replacement of enriched subcontinental lithospheric mantle by underlying depleted asthenosphere has also been proposed for the incipient rift in Afar, Ethiopia ([42,43] and references therein). To account for isotopic variations along the complete section of the Afro-Arabian rift system Schilling et al. [44] involved the interaction of a thermal HIMU-type mantle plume beneath Afar with depleted asthenosphere and overlying EM-type mantle lithosphere. Clearly, the Afar example can be envisaged as a close analogue to the RSR. It follows that mantle composition, structure and evolution beneath the RSR in Northern Victoria Land are comparable to other continental settings.

Another question concerns the origin of the HIMU component: Is it lithospheric or plume-derived? Several factors favour a plume origin for the HIMU-like signature: (1) its ubiquity in RSR rocks from various structural settings and different plate tectonic domains suggests an origin which is originally unrelated to the lithosphere, (2) its longevity in MBL-shoulder rocks for more than 24 Ma indicates a mantle source which has

never been consumed, and (3) the analogy to modern HIMU plumes [24]. The question arises as to whether the HIMU component represents one or more active plumes related to Ross Sea rifting or whether the plume may have become ‘fossilized’ in the sense of the Stein and Hofmann model [45] (i.e., whether it became part of the rigid lithospheric mantle long before rifting).

Recent models for the dynamics of mantle plumes have shown that plume heads driven by thermal buoyancy will entrain surrounding cooler mantle during ascent, the result of which will be an increase in the size of the plume, a decrease in temperature, and a heterogeneous and ‘contaminated’ composition [46,47]. In contrast, the narrow feeder conduit following the plume head will consist of uncontaminated and hotter source material, causing a significant temperature gradient between central and peripheral parts of the plume head. After impinging on the base of the lithosphere the plume head will be flattened and again enlarged by a factor of two. A ‘contaminated’ and flattened plume head at the base of the lithosphere could explain why the magmas from the within-rift, TAM shoulder and MBL localities have the HIMU-type end member in common. It could further explain why the composition of this component is intermediate between that of HIMU and MORB mantle. Moreover, it is also consistent with the seemingly limited vertical extent of the HIMU-type mantle beneath the rift trough (and probably also beneath the TAM) which is indicated by the relatively fast replacement of HIMU-type by MORB-type signatures in within-rift basalts. Apart from the RSR and MBL areas, HIMU-type mantle components (plumes?) exist beneath the Balleny Islands and even in Tasmania and the Campbell Plateau on the opposite side of the southern Pacific [30]. Three interpretations are possible:

(1) The HIMU component represents one single large plume [8,48] actively involved in Ross Sea Rifting. In this case the HIMU signatures in the Balleny Islands, Tasmania and Campbell Plateau would be unrelated.

(2) HIMU signatures in Antarctica and the adjacent southern Pacific regions are all related by a series of smaller active plumes, all of which

are of HIMU type. In this case this ‘swarm’ of plumes should represent a very large, deep mantle reservoir.

(3) The HIMU signature represents an old ‘fossilized’ plume head [45] which would have to be older than breakup between Antarctica, Australia and New Zealand.

The existence of several presently active, supposed (HIMU) plume-related volcanic provinces (Balleny Islands, MBL and Mt. Erebus [3,4,18,28,30,48,49]) is consistent with the plume-swarm hypothesis. On the other hand, the apparent limited vertical extent of the HIMU-type mantle favours the ‘fossilized’ plume head hypothesis. The appearance of HIMU–PREMA-like signatures beneath different segments of former Gondwanaland (Arabian plate, East Africa and Antarctica (e.g., [30,44,45]) would then suggest that ‘fossilized’ plumes played an important role in the formation of these continents.

8. Conclusions

New Sr-Nd-Pb isotope and trace element data for Cenozoic near-primary basalts from the Ross Sea Rift, western Antarctica, in conjunction with data from the literature for other Ross Sea Rift basalts, suggest the involvement of three mantle source components (or their mixtures) during the formation of rift-related magmas: depleted asthenospheric mantle (DMM or PREMA), an enriched mantle component (EM), and a component akin to HIMU. The involvement of these mantle components during magma genesis correlates with tectonic setting and rift evolution: where rifting has progressed furthest, as in the vicinity of the Victoria Land Basin, the mantle sources appear to be isotopically most depleted. Consequently, MORB-type signatures are restricted to Recent within-rift basalts. In contrast, EM signatures are restricted to basalts from the western rift shoulder (Transantarctic Mountain Range). Temporal isotopic and trace element variations are observed both for within-rift and off-rift basalts. Basalts from the western rift shoulder evolved from EM- towards HIMU-type signatures between 15 and 5 Ma. The within-rift

and Marie Byrd Land basalts changed from HIMU- towards MORB-type signatures from 8 Ma and 14 Ma onwards respectively.

These observations suggest progressive replacement of EM- by HIMU-type sources (western rift shoulder) and of HIMU- by MORB-type mantle sources (within-rift setting and Marie Byrd Land) during rift evolution and argue for an upper mantle stratified in the order MORB- to HIMU- to EM-type sources. In this model, the EM source component is likely to reside in the subcontinental lithosphere because of its restriction to the rift shoulder environment and its progressive consumption during rifting. In contrast the MORB-type mantle represents depleted asthenosphere which is increasingly involved in magma genesis where rifting has advanced most (i.e., in the immediate surroundings of the Victoria Land Basin). The HIMU-type component may be related to a flattened head of an active or, alternatively, 'fossilized' mantle plume attached to the base of the lithosphere.

Similar transitions from lithospheric to asthenospheric mantle sources during rifting have been observed for the Rio Grande Rift and for the Red Sea–Gulf of Aden and Tadjoura–Asal Rift area [33,38–40,42–44]. None of the recognized mantle components has the highly enriched isotopic signature proposed for the source of the Jurassic Ferrar igneous rocks [31]. This either suggests that sediment-subduction-modified [31] mantle was not tapped during Ross Sea Rift magmatism, or that crustal contamination has caused the unusual geochemical signature of the Ferrar rocks. Finally, the appearance of HIMU-like signatures beneath different segments of former Gondwanaland (Arabian plate, East Africa and Antarctica [30,44,45]) suggests that 'fossilized' plumes played an important role in the formation of these continents.

Acknowledgements

We thank I. Hornig and M. Schmidt-Thomé for providing samples collected during the GANOVEX VI expedition. We are also grateful to R. Altherr, A. Hofmann, T. Reischmann and

F. Volker for critical comments and suggestions. Constructive reviews by J.G. Fitton, K. Hoernle, P.R. Kyle, S.-S. Sun and M.-C. Williamson greatly helped to improve this paper. Financial and logistic support was provided by DFG grant Wo 362/3, the *Bundesanstalt für Geowissenschaften und Rohstoffe* and the *Alfred-Wegener-Institut*. [CL]

References

- [1] G. Wörner, H. Niephaus, J. Hertogen and L. Viereck, The Mt. Melbourne Volcanic Field (Victoria Land, Antarctica) II: Geochemistry and magma genesis, *Geol. Jahrb.* E38, 395–433, 1989.
- [2] K. Futa and W. LeMasurier, Nd and Sr isotopic studies on Cenozoic mafic lavas from West Antarctica: Another source for continental alkali basalts, *Contrib. Mineral. Petrol.* 83, 38–44, 1983.
- [3] M.J. Hole and W.E. LeMasurier, Tectonic controls on geochemical compositions of Cenozoic mafic alkaline volcanic rocks from West Antarctica, *Contrib. Mineral. Petrol.* 117, 187–202, 1994.
- [4] S.-S. Sun and G.N. Hanson, Origin of Ross Island basanitoids and limitations upon the heterogeneity of mantle sources for alkali basalts and nephelinites, *Contrib. Mineral. Petrol.* 52, 77–106, 1975.
- [5] C.J. Allègre, B. Dupré, B. Lambert and P. Richard, The subcontinental versus suboceanic debate, I. Lead–neodymium–strontium isotopes in primary alkali basalts from a shield area: The Ahaggar volcanic suite, *Earth Planet. Sci. Lett.* 52, 85–92, 1981.
- [6] J.C. Behrendt, W. LeMasurier, A. Cooper, F. Tessensohn, A. Trehu and D. Damaske, Geophysical studies of the West Antarctic rift system, *Tectonics* 10(6), 1257–1273, 1991.
- [7] A.K. Cooper, F.J. Davey and J.C. Behrendt, Seismic stratigraphy and structure of the Victoria Land basin, Western Ross Sea, Antarctica, in: *The Antarctic Continental Margin: Geology and Geophysics of the Western Ross Sea* (Circum-Pac. Coun. Energy Miner. Resour. Earth Sci. Ser. 5B), pp. 27–76, 1987.
- [8] J.C. Behrendt, D.D. Blankenship, C.A. Finn, R.E. Bell, S.M. Sweeney and J.M. Brozena, CASERTZ aeromagnetic data reveal Late Cenozoic flood basalts(?) in the West Antarctic Rift System, *Geology* 22, 481–576, 1994.
- [9] F. Tessensohn and G. Wörner, The Ross Sea Rift system: Structure, evolution and analogues, in: *Geological Evolution of Antarctica*, M.R.A. Thomson, J.A. Crame and J.W. Thomson, eds., pp. 273–278, Cambridge University Press, Cambridge, U.K., 1991.
- [10] P. van der Beek, S. Cloetingh and P. Andriessen, Mechanisms of extensional basin formation and vertical motions at rift flanks: Constraints from tectonic modelling and fission-track thermochronology, *Earth Planet. Sci. Lett.* 121, 417–433, 1994.

- [11] P.G. Fitzgerald, M. Sandiford, P.J. Barrett and A.J.W. Gleadow, Asymmetric extension associated with uplift and subsidence in the Transantarctic Mountains and Ross Sea Embayment, *Earth Planet. Sci. Lett.* 81, 67–78, 1987.
- [12] P. Müller, M. Schmidt-Thomé, H. Kreuzer, F. Tessensohn and U. Vetter, Cenozoic peralkaline magmatism at the western margin of the Ross Sea, Antarctica, *Mem. Soc. Geol. Ital.* 46, 315–336, 1991.
- [13] P. Armienti, L. Civetta, F. Innocenti, P. Manetti, A. Tripodo, L. Villari and G. Vita, New petrological and geochemical data on Mt. Melbourne Volcanic Field, Northern Victoria Land, Antarctica (II Italian Antarctic Expedition), *Mem. Soc. Geol. Ital.* 46, 397–424, 1991.
- [14] I. Hornig and G. Wörner, Cenozoic volcanics from Coulman Island, Mandible Cirque, Malta Plateau and Navigator Nunatak, Victoria Land, Antarctica, *Geol. Jahrb.*, in press.
- [15] J.C. Behrendt and D. Cooper, Evidence for rapid uplift of the shoulder escarpment of the West Antarctic rift system and speculation on possible climate forcing, *Geology* 19, 315–319, 1991.
- [16] J.C. Behrendt, H.J. Duerbaum, D. Damaske, R. Saltus, W. Bosum and A. Cooper, Extensive volcanism and related tectonism beneath the western Ross Sea continental shelf, Antarctica: Interpretation of an aeromagnetic survey, in: *Geological Evolution of Antarctica*, M.R.A. Thompson, J.A. Crame and J.W. Thomson, eds., pp. 299–304, Cambridge University Press, Cambridge, U.K., 1991.
- [17] I.W.D. Dalziel, Antarctica: a tale of two supercontinents?, *Annu. Rev. Earth Planet. Sci.* 20, 501–526, 1992.
- [18] P.R. Kyle, McMurdo Volcanic Group, introduction, in: *Volcanoes of the Antarctic Plate and Southern Oceans*, W.E. LeMasurier and J.W. Thomson, eds., *Am. Geophys. Union Antarct. Res. Ser.* 48, 19–25, 1990.
- [19] F.A. Frey, D.H. Green and S.D. Roy, Integrated models of basalt petrogenesis: a study of quartz tholeiites to olivine melilitites from south-eastern Australia utilizing geochemical and experimental petrological data, *J. Petrol.* 19, 463–513, 1978.
- [20] I. Hornig, G. Wörner and J. Zipfel, Lower crustal and mantle xenoliths from the Mt. Melbourne Volcanic Field, Northern Victoria Land, Antarctica, *Mem. Soc. Geol. Ital.* 46, 337–352, 1992.
- [21] W. White and J. Patchett, Hf-Nd-Sr isotopes and incompatible element abundances in island arcs: implications for magma origin and crust–mantle evolution, *Earth Planet. Sci. Lett.* 67, 167–185, 1984.
- [22] B.D. Taras and S.R. Hart, Geochemical evolution of the New England seamount chain: isotopic and trace-element constraints, *Chem. Geol.* 64, 35–54, 1987.
- [23] G. Wörner, A. Zindler, H. Staudigel and H.U. Schmincke, Sr, Nd and Pb isotope geochemistry of Tertiary and Quarternary alkaline volcanics from West Germany, *Earth Planet. Sci. Lett.* 79, 107–119, 1986.
- [24] A. Zindler and S.R. Hart, Chemical geodynamics, *Annu. Rev. Earth Planet. Sci.* 14, 493–571, 1986.
- [25] S.R. Taylor and S.C. McLennan, *The Continental Crust: Its Composition and Evolution*, Blackwell, Oxford, U.K., 1985.
- [26] B.L. Weaver and J. Tarney, Empirical approach to estimating the composition of the continental crust, *Nature* 310(5978), 575–577, 1984.
- [27] B.L. Weaver, Trace element evidence for the origin of ocean-island basalts, *Geology* 19, 123–126, 1991.
- [28] S.R. Hart and P.R. Kyle, The geochemistry of McMurdo Group volcanic rocks, *Antarct. J. U.S.* 28, 14–16, 1994.
- [29] S.R. Hart, Heterogeneous mantle domains: signatures, genesis and mixing chronologies, *Earth Planet. Sci. Lett.* 90, 273–296, 1988.
- [30] R. Lanyon, R. Varne and A.J. Crawford, Tasmanian Tertiary basalts, the Balleny plume and opening of the Tasman Sea–southwest Pacific Ocean, *Geology* 21(5), 555–558, 1993.
- [31] J.M. Hergt, B.W. Chappell, G. Faure and T.M. Mensing, The geochemistry of Jurassic dolerites from Portal Peak, Antarctica, *Contrib. Mineral. Petrol.* 102, 298–305, 1989.
- [32] S.-S. Sun and W.F. McDonough, Chemical and isotopic systematics of oceanic basalts: implications for mantle composition and processes, in: *Magmatism in the Ocean Basins*, A.D. Saunders and M.J. Norry, eds., *Geol. Soc. London Spec. Publ.* 42, 313–345, 1989.
- [33] J.G. Fitton, D. James and W.P. Leeman, Basic magmatism associated with Late Cenozoic extension in the western United States: Compositional variations in space and time, *J. Geophys. Res.* 96(B8), 13693–13711, 1991.
- [34] J.G. Fitton, D. James, P.D. Kempton, D.S. Ormerod and W.P. Leeman, The role of lithospheric mantle in the generation of Late Cenozoic basic magmas in the western United States, *J. Petrol., Spec. Lithosphere Iss.*, pp. 331–349, 1988.
- [35] M. Tatsumoto, A.R. Basu, H. Wankang, W. Junwen and X. Guanhong, Sr, Nd, and Pb isotopes of ultramafic xenoliths in volcanic rocks from Eastern China: enriched components EMI and EMII in subcontinental lithosphere, *Earth Planet. Sci. Lett.* 113, 107–128, 1992.
- [36] M.A. Menzies and P.R. Kyle, Continental volcanism: A crust–mantle probe, in: *Continental Mantle*, M.A. Menzies, ed., pp. 157–177, Clarendon, Oxford, 1990.
- [37] M.A. Menzies, Archean, Proterozoic, and Phanerozoic lithospheres, in: *Continental Mantle*, M.A. Menzies, ed., pp. 67–86, Clarendon, Oxford, 1990.
- [38] F.V. Perry, W.S. Baldrige and D.J. DePaolo, Chemical and isotopic evidence for lithospheric thinning beneath the Rio Grande rift, *Nature* 332, 432–434, 1988.
- [39] T.K. Bradshaw, C.J. Hawkesworth and K. Gallagher, Basaltic volcanism in the southern Basin and Range: no role for a mantle plume, *Earth Planet. Sci. Lett.* 116, 45–62, 1993.
- [40] M.A. Menzies and P.R. Kyle, Enriched and depleted source components for tholeiitic and alkaline lavas from

- Zuni–Bandera, New Mexico: Inferences about intraplate processes and stratified lithosphere, *J. Geophys. Res.* 96(B8), 13645–13671, 1991.
- [41] K. Hoernle, G. Tilton and H.-U. Schmincke, Sr-Nd-Pb isotopic evolution of Gran Canaria: evidence for shallow enriched mantle beneath the Canary Islands, *Earth Planet. Sci. Lett.* 106, 44–63, 1991.
- [42] P.J. Betton and L. Civetta, Sr and Nd isotopic evidence for the heterogeneous nature and development of the mantle beneath Afar (Ethiopia), *Earth Planet. Sci. Lett.* 71, 59–70, 1984.
- [43] W.K. Hart, G. WoldeGabriel, R.C. Walter and S.A. Mertzman, Basaltic volcanism in Ethiopia: Constraints on continental rifting and mantle interactions, *J. Geophys. Res.* 94, 7731–7748, 1989.
- [44] J.-G. Schilling and R.H. Kingsley, Nd-Sr-Pb isotopic variations along the Gulf of Aden: Evidence for Afar mantle plume–continental lithosphere interaction, *J. Geophys. Res.* 97(B7), 10927–10966, 1992.
- [45] M. Stein and A.W. Hofmann, Fossil plume head beneath the Arabian lithosphere?, *Earth Planet. Sci. Lett.* 114, 193–209, 1992.
- [46] R.W. Griffiths and I.H. Campbell, Stirring and structure in mantle starting plumes, *Earth Planet. Sci. Lett.* 99, 66–78, 1990.
- [47] J.A. Whitehead and D.S. Luther, Dynamics of laboratory diapir and plume models, *J. Geophys. Res.* 80, 705–717, 1975.
- [48] J.C. Behrendt, W.E. LeMasurier and A.K. Cooper, The West Antarctic Rift System—a propagating rift ‘captured’ by a mantle plume, in: *Recent Progress in Antarctic Earth Sciences*, K. Kaminuma and Y. Yoshida, eds., pp. 315–322, Terra, Tokyo, 1992.
- [49] P.R. Kyle, J.A. Moore and M.F. Thirlwall, Petrologic evolution of anorthoclase phonolite lavas at Mount Erebus, Ross Island, Antarctica, *J. Petrol.* 33, 849–875, 1992.
- [50] W. Todt, R.A. Cliff, A. Hanser and A.W. Hofmann, $^{202}\text{Pb} + ^{205}\text{Pb}$ spike for lead isotopic analysis, *Terra Cognita* 4, 209, 1984 (Abstr.).